

## Corrosion behaviors of arc spraying single and double layer coatings in simulated Dagang soil solution

LIN Bi-lan(林碧兰)<sup>1</sup>, LU Xin-ying(路新瀛)<sup>1</sup>, LI Long(李 龙)<sup>2</sup>

1. Graduate School at Shenzhen, Tsinghua University, Shenzhen 518055, China;

2. Guangdong Sanhe Pipe-pile Co. Ltd., Zhongshan 518424, China

Received 10 August 2009; accepted 15 September 2009

**Abstract:** Three kinds of single layer coatings of Zn, Zn15Al, 316L stainless steel and two kinds of double layer coatings with inner layer of Zn or Zn15Al and outer layer of 316L stainless steel by arc spraying were developed to protect the metal ends of prestressed high-strength concrete (PHC) pipe piles against soil corrosion. The corrosion behaviors of the coated Q235 steel samples in the simulated Dagang soil solution were investigated by potentiodynamic polarization, electrochemical impedance spectroscopy (EIS) and natural immersion tests. The results show that the corrosion of the matrix Q235 steel is effectively inhibited by Zn, Zn15Al, Zn+316L and Zn15Al+316L coatings. The corrosion rate value of Zn15Al coated samples is negative. The corrosion products on Zn and Zn15Al coated samples are compact and firm. The corrosion resistance indexes of both Zn and Zn15Al coated samples are improved significantly with corrosion time, and the latter are more outstanding than the former. But the corrosion resistance of 316L coated samples is decreased quickly with the increase in immersion time. When the coatings are sealed with epoxy resin, the corrosion resistance of the coatings will be enhanced significantly.

**Key words:** arc spraying; coating; corrosion behavior; soil corrosion; PHC pipe pile; zinc; stainless steel

### 1 Introduction

PHC pipe piles have been widely applied in aggressive environment such as offshores and ports, where their durability is demanded to be more and more strict[1–2]. The durability of PHC pipe piles at least includes the durability of the pile body and the metal ends. The durable techniques of the body concrete have been put forward, but those of the metal ends have less been reported yet. The metal ends of PHC pipe piles are composed of apron, end plate and pretensioned PC bar of which the materials and the compositions are different. In corrosive soil, various corrosion such as chemical, electrochemical and galvanic corrosion will occur[3–4]. The safety of the engineering structure might thus be affected, which requires a corrosion protection before serving.

Arc spraying metal coatings have been widely applied to the engineering of the corrosion protection[5–8]. Stainless steel coatings are wear resistant and have long-term protection. Zinc, aluminum

and zinc-aluminum alloy coatings can be acted as both physical barriers and sacrificial anodes, and their corrosion products are protective.

In this work, three kinds of single layer coatings of Zn, Zn15Al, 316L stainless steel and two kinds of double layer coatings with inner layer of Zn or Zn15Al and outer layer of 316L by arc spraying were invited to protect the metal ends of PHC pipe piles against soil corrosion. The corrosion behaviors of the coated Q235 steel samples in the simulated solution of Dagang chloride salt soil were investigated.

### 2 Experimental

The matrix material was cold-rolled Q235 steel. Zn, Zn15Al and 316L with 2 mm in diameter were selected as the spraying materials. Zn15Al contains 85% Zn and 15% Al (mass fraction). The processing parameters of arc spraying for Zn and Zn15Al coatings were as follows: spray voltage 28 V, spray current 200 A, spray distance 200 mm and air pressure 0.65 MPa. And the corresponding parameters for 316L coatings were as

follows: 32 V, 260 A, 200 mm and 0.65 MPa, respectively. Five kinds of arc spraying coatings were developed: three types of single layer coatings of Zn, Zn15Al, 316L, and two types of double layer coatings with inner layer of Zn or Zn15Al and outer layer of 316L. The total thickness of the metal coatings was about 160  $\mu\text{m}$ , and for double layer coatings the thickness of each layer was about 80  $\mu\text{m}$ .

The compositions of the simulated chloride salt soil in Dagang were 18.04 g/L NaCl and 1.66 g/L  $\text{Na}_2\text{SO}_4$ . The pH value was 8.6. The solutions were prepared from reagent grade chemicals and de-ionized water.

Potentiodynamic polarization and EIS measurements were carried out under galvanostatic condition using a potentiostat/galvanostat response analyzer of electrochemical workstation (Model: CS360) with a conventional three-electrode cell system. A saturated calomel electrode (SCE) was used as a reference electrode. A platinum electrode with an area of 10  $\text{cm}^2$  was served as an auxiliary electrode. The exposed area of the working electrode was 10 mm  $\times$  10 mm. Before electrochemical measurements, a steady potential was obtained. The scan rate for polarization was 1 mV/s. EIS measurements were performed at corrosion potential in the frequency range between 100 kHz and 0.01 Hz with a potential sine signal of 10 mV. All electrochemical measurements were carried out in a nondeaerated simulated solution at room temperature. The EIS diagrams were fitted by Zview soft.

The corrosion rate of the samples was determined by mass loss during immersion. The weighing accuracy is 0.1 mg.

To sign the samples with different coatings, the symbols are introduced as follows: Zn, coated with pure Zn; Zn15Al, coated with Zn15Al alloy; 316L, coated with 316L stainless steel; Zn+316L, coated with inner layer of Zn and outer layer of 316L stainless steel; and Zn15Al+316L, coated with inner layer of Zn15Al alloy and outer layer of 316L stainless steel.

### 3 Results and discussion

#### 3.1 Corrosion rate of coated samples

The red rusts presented on the surface of 316L after immersion in simulated soil solution for one day, and a loose and thick layer of red rusts were shown after immersion for 30 d. While the corrosion of the matrix Q235 steel was effectively inhibited by other four types of coatings on which white rusts were only observed after immersion for 110 d.

For two kinds of double layer coated samples, the outer layer of 316L bubbled and warped when they were immersed in simulated soil solution for 30 d. The outer layer of 316L coatings by arc spraying was coarse and

porous[9]. The corrosive media such as chloride ions, sulfate ions and oxygen might diffuse to the surface of the inner layer of Zn or Zn15Al coatings. The galvanic corrosion systems thus might be formed. 316L acted as cathode, while Zn or Zn15Al served as anode. The volume of the corrosion products of Zn and Zn15Al was greater than that of Zn and Zn15Al, and the internal stress was generated. Therefore, the outer layer of 316L coatings was upwarped.

When these five kinds of metal coatings were sealed with epoxy resin about 120  $\mu\text{m}$  in thickness, the appearance of the whole coatings almost kept unchanged after immersion for 110 d.

Fig.1 shows the corrosion rate of three kinds of single layer coated samples after immersion for 30 d and 50 d (because the outer layer of 316L warped during corrosion, the errors of the corrosion rate calculated by mass loss is very great). The corrosion rate of Zn coated samples is decreased with the increase in immersion time. This may be due to the fact that: 1) the pores of Zn coatings may be filled with the corrosion products during corrosion which are impossible to be removed[10–11]; and 2) the corrosion products on the surface not only become compact and thick, but also are combined with Zn coatings firmly which are difficult to be removed. The corrosion rate value of Zn15Al coated samples is negative, suggesting that the corrosion products on Zn15Al coatings are more compact and more difficult to be removed than those on Zn coatings[10]. However, the corrosion rate of 316L coated samples is increased with the increase in immersion time.

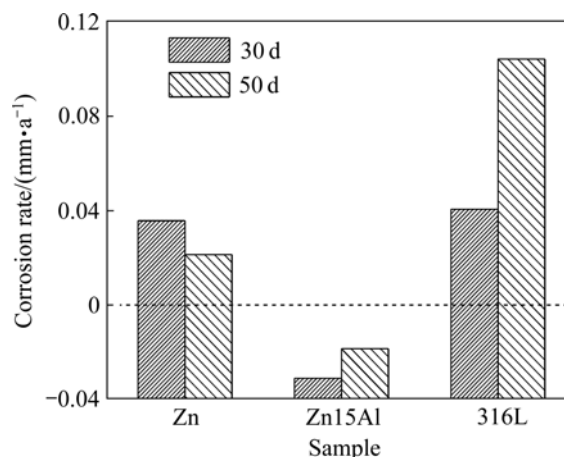
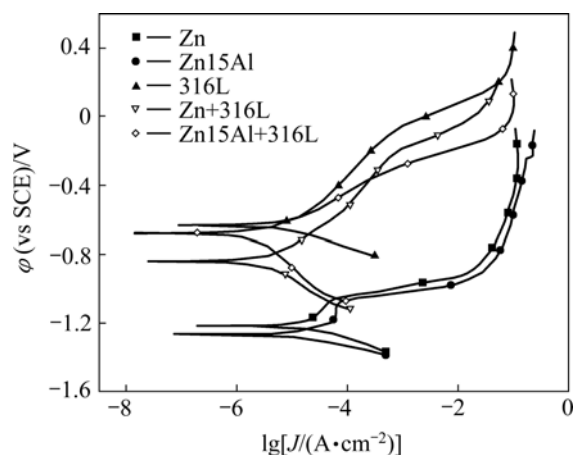


Fig.1 Corrosion rate of Zn, Zn15Al, 316L coated samples immersed in simulated solution for 30 d and 50 d

#### 3.2 Electrochemical corrosion behaviors of coated samples

The polarization curves for five kinds of coated Q235 steel samples immersed in simulated soil solution for 30 min are shown in Fig.2. The cathodic process of all samples is controlled by activation polarization, while

that of Q235 steel is controlled by oxygen diffusion[4]. The anodic and cathodic processes of 316L, Zn+316L and Zn15Al+316L are suppressed more markedly than those of Zn and Zn15Al, and the corrosion potential of the three former ones is more positive than those of the two latter ones.



**Fig.2** Polarization curves for five kinds of coated Q235 steel samples immersed in simulated soil solution for 30 min

In general, the left shift of the anodic or cathodic branches on the polarization curve indicates that at the same polarization potential the polarization current is decreased and the corresponding corrosion process is suppressed, and vice versa.

As shown in Fig.2, the anodic processes of Zn and Zn15Al coated samples are nearly similar. There is a passivation region between +75 mV and +200 mV related to  $\phi_{\text{corr}}$ , but for a higher polarization potential the current density of Zn and Zn15Al coatings increases with potential quickly where the anodic process is the dissolution of Zn or Al. Compared with Zn15Al coated sample, the anodic branch of Zn coated sample is left-shifted slightly. Moreover, the corrosion potential of Zn is slightly larger than that of Zn15Al because 15% (mass fraction) of Al, of which the corrosion potential is exceedingly negative and will be corroded more easily, is present in Zn15Al alloy.

The shapes of the polarization curves for 316L, Zn+316L and Zn15Al+316L are approximately similar, and both the cathodic and anodic processes of the samples are controlled by activation polarization, as shown in Fig.2. The anodic process of 316L is inhibited more greatly than that of Zn+316L or Zn15Al+316L, but the cathodic processes of the two latter ones are prohibited more markedly than these of the former. The corrosion potential of 316L is higher than that of Zn+316L or Zn15Al+316L. These can be ascribed to the porosity of 316L coatings and the dissolution of the inner layer of Zn or Al.

The polarization curves for Zn, Zn15Al, 316L and Zn+316L immersed in simulated soil solution for different time are shown in Fig.3. And the corresponding corrosion potential  $\phi_{\text{corr}}$ , corrosion current density  $J_{\text{corr}}$ , polarization resistance  $R_p$ , cathodic Tafel constant  $b_c$  and anodic Tafel constant  $b_a$ , are listed in Table 1.

As shown in Fig.3(a), the anodic branch of Zn is left-shifted greatly with the increase in corrosion time from 30 min to 30 d, but the anodic passivation region disappears and the cathodic branch is right-shifted markedly. When the corrosion time is increased to 50 d, the anodic branch continues to shift left and a slight passivation region presents again; and the cathodic branch is left-shifted greatly. In a longer corrosion time, the anodic branch is almost unchanged, but the cathodic branch is still left-shifted.

As shown in Fig.3(b), the change law of the anodic branches of Zn15Al is almost the same as that of Zn. The cathodic branch of Zn15Al is also left-shifted with the increase in corrosion time from 30 min to 30 d but appears to be unchanged for a longer immersion time.

Extending the corrosion time from 30 min to 30 d, both the anodic and cathodic branches of 316L are shifted obviously in the right direction, as shown in Fig.3(c). Prolonging the corrosion time, the polarization branches are almost invariant.

In Fig.3(d), with prolonging the corrosion time, the anodic branch of Zn+316L is left-shifted while the cathodic branch is right-shifted. The change law of Zn15Al+316L is nearly similar to that of Zn+316L, so their polarization curves are omitted in this work.

In Table 1, for Zn, compared with the corrosion time of 30 min,  $\phi_{\text{corr}}$  value becomes positive obviously;  $J_{\text{corr}}$  is decreased for about one order of magnitude;  $R_p$  value is increased conspicuously; and the values of  $b_a$  and  $b_c$  are increased. It is indicated that the corrosion resistance indexes of Zn after immersion are improved remarkably. Moreover, with prolonging the corrosion time, the corrosion resistance indexes almost keep improving. By the increase of  $b_a$  and  $b_c$  values with corrosion time, it can be also considered that the corrosion products of Zn are compact and fasten which can effectively inhibit the dissolution of Zn and the reduction reaction of oxygen.

As shown in Table 1, the change law of the corrosion resistance indexes of Zn15Al with corrosion time is almost the same as that of Zn. And the corrosion resistance indexes of Zn15Al are more outstanding than those of Zn.

As far as 316L coated samples are considered, the corrosion resistance indexes are decreased obviously with the increase in corrosion time from 30 min to 30 d, and remain to be poor for a longer corrosion time, as shown in Table 1. For double layer coatings, the corrosion

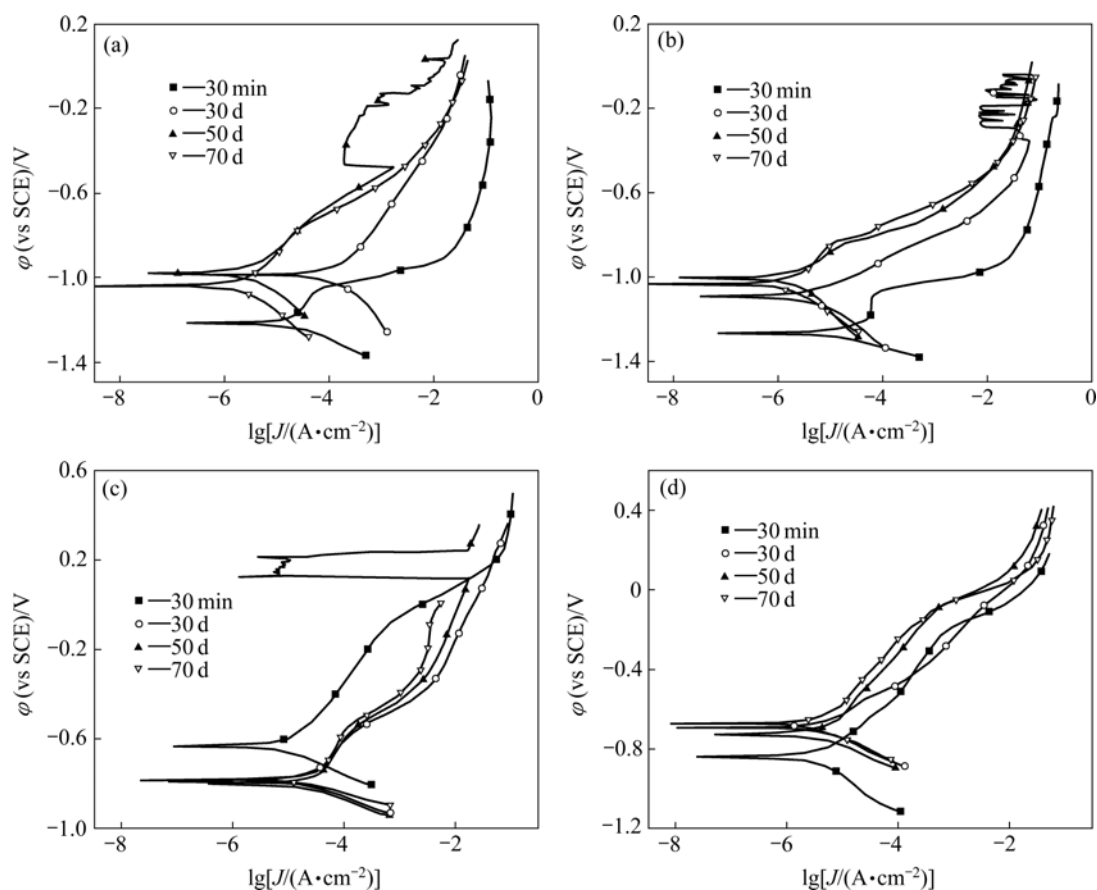


**Fig.3** Polarization curves for arc spraying Zn (a), Zn15Al (b), 316L (c) and Zn+316L (d) coated samples immersed in simulated soil solution for different time

**Table 1** Corrosion potential  $\varphi_{\text{corr}}$ , corrosion current density  $J_{\text{corr}}$ , polarization resistance  $R_p$ , anodic Tafel constant  $b_a$  and cathodic Tafel constant  $b_c$  obtained from Fig.3

Sample	Corrosion time	$\varphi_{\text{corr}}(\text{vs SCE})/\text{V}$	$J_{\text{corr}}/(\mu\text{A}\cdot\text{cm}^{-2})$	$R_p/(\Omega\cdot\text{cm}^{-2})$	$b_a/\text{mV}$	$b_c/\text{mV}$
Zn	30 min	-1.215	21.1	1 238	86	152
	30 d	-0.986	2.2	3 225	103	97
	50 d	-0.977	2.0	10 923	332	273
	70 d	-1.037	1.7	14 867	422	297
Zn15Al	30 min	-1.267	18.5	1 411	185	73
	30 d	-1.090	3.8	6 873	115	149
	50 d	-1.005	1.6	16 256	275	370
	70 d	-1.032	1.3	19 677	320	241
316L	30 min	-0.633	7.6	3 425	296	141
	30 d	-0.788	24.1	1 080	410	126
	50 d	-0.800	24.2	1 078	394	122
	70 d	-0.786	27.2	958	415	96
Zn+316L	30 min	-0.838	2.7	9 818	286	312
	30 d	-0.690	4.5	5 846	301	185
	50 d	-0.724	3.7	7 039	255	132
	70 d	-0.673	3.1	8 482	584	241
Zn15Al+ 316L	30 min	-0.678	1.8	14 545	122	323
	30 d	-0.696	4.7	5 576	478	223
	50 d	-0.788	2.8	9 157	377	289
	70 d	-0.894	4.1	6 422	492	224

resistance indexes are fluctuated with corrosion time.

Fig.4 presents the electrochemical impedance diagrams for Zn15Al immersed in simulated soil solution for different time. With extending the corrosion time, the size of the diagrams is increased evidently. It is suggested that the impedance value of Zn15Al is increased with corrosion time significantly.

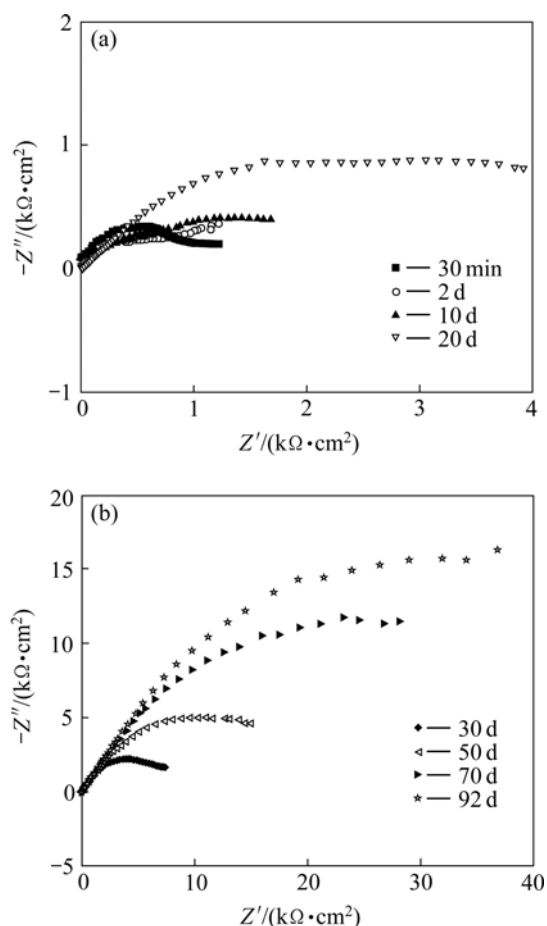


**Fig.4** Electrochemical impedance diagrams for Zn15Al immersed in simulated soil solution for different time

As shown in Fig.4, these diagrams contain two time constants corresponding to high frequency capacitive loop (HFCL) and low frequency capacitive loop (LFCL). The EIS diagrams for Zn almost are similar to those of Zn15Al. In the case of a shorter corrosion time, HFCL can be attributed to the pores of the arc spraying coatings. For a longer corrosion time, HFCL can be ascribed to the corrosion products of Zn15Al. LFCL can be attributed to the electric double layer of the solution/substrate interface[10–11].

The diagrams in Fig.4 can be described by the equivalent circuit shown in Fig.5.  $R_s$  is the solution resistance; CPEr is the constant-phase element depicting the capacitance of the spraying coatings or the corrosion products at HFCL;  $R_r$  is the resistance of the pores of the spraying coatings or the corrosion products; CPEdl is the constant-phase element denoting the electric double layer

of the solution/substrate interface at LFCL; and  $R_{ct}$  is the charge transfer resistance. Here, CPE has an impedance dispersion relation of  $Q=1/Y_0(j\omega)^n$ . If  $n=1$ , 0 or  $-1$ , the CPE represents a capacitance ( $C$ ), a resistance ( $R$ ) or an inductance ( $L$ ), respectively[12].

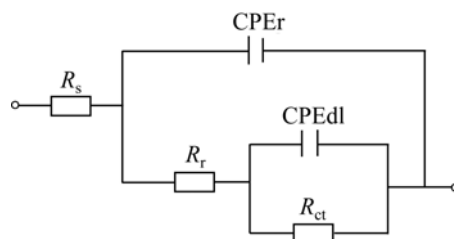


**Fig.5** Equivalent circuit for Zn15Al coated samples immersed in simulated soil solutions for different time

The electrochemical corrosion parameters of  $Y_0$ -CPEdl,  $n$ -CPEdl and  $R_{ct}$  at LFCL for Zn15Al and Zn fitted by Fig.5 are listed in Table 2. As shown in Table 2, the value of  $n$  is in the range of  $0 < n < 1$ . It thus can be suggested that the electric double layer of solution/substrate interface is dispersed, which leads to the depression of the capacitance. Here  $n$  can be expressed as[13–14]

$$n = 1 - 2\alpha / 180 \quad (1)$$

where  $\alpha$  is the depression angle. Thus  $n$  denotes the uniformity of the surface of the capacitance which is directly related to the coverage and compactness of the spraying coatings or the corrosion products. The larger the  $n$  value is, the more compact and uniform the coatings are.

**Table 2** Corrosion parameters of  $Y_0$ -CPEdl,  $n_0$ -CPEdl and  $R_{ct}$  at LFCL for coated samples fitted by equivalent circuit in Fig.5

Sample	Corrosion time	$Y_0$ -CPEdl/ ( $\Omega^{-1} \cdot \text{cm}^{-2} \cdot \text{s}^{-n}$ )	$n$ -CPEdl	$R_{ct}$ / ( $\Omega \cdot \text{cm}^2$ )
Zn15Al	30 min	$1.976 \times 10^{-4}$	0.706	1 130
	2 d	$6.022 \times 10^{-4}$	0.544	1 282
	10 d	$4.971 \times 10^{-4}$	0.429	2 062
	20 d	$1.727 \times 10^{-4}$	0.496	4 554
	30d	$1.084 \times 10^{-4}$	0.541	9 266
	50 d	$0.887 6 \times 10^{-4}$	0.544	22 843
	70 d	$0.713 4 \times 10^{-4}$	0.545	57 454
	92 d	$0.685 1 \times 10^{-4}$	0.563	79 602
Zn	30 min	$2.924 \times 10^{-4}$	0.805	493
	2 d	$16.23 \times 10^{-4}$	0.461	685
	10 d	$2.669 \times 10^{-4}$	0.428	2 990
	20 d	$1.434 \times 10^{-4}$	0.437	8 994
	30d	$1.384 \times 10^{-4}$	0.407	15 706
	50 d	$1.242 \times 10^{-4}$	0.386	19 190
	70 d	$1.062 \times 10^{-4}$	0.352	20 076
	92 d	$1.140 \times 10^{-4}$	0.390	13 052

The capacitance value is proportional to the dielectric constant and surface area, and is inverse proportional to the distance of the two layer of the capacitance[15]. When the surface of the spraying coatings is covered with the corrosion products, the dielectric constant of the capacitance will be decreased[12]. The more compact the corrosion products are, the smaller the surface area of the capacitance is. The thicker the corrosion products are, the longer the distance between the two layers of the capacitance is. Therefore, the smaller the  $Y_0$ -CPedl value is, the thicker and more compact the corrosion products may be.

The thicker and more compact the corrosion products are, the more difficult the charge transfer is. As far as Zn15Al is concerned, with the increase in corrosion time, the  $Y_0$ -CPedl value is decreased; the  $n_0$ -CPedl value is increased; and  $R_{ct}$  value is increased remarkably, as shown in Table 2. It thus can be considered that the corrosion products on the surface of Zn15Al become more and more thick and compact with corrosion time.

In Table 2, the corrosion resistance indexes of Zn are improved with the increase in corrosion time from 30 min to 70 d but appear to be slightly poor in a longer corrosion time.

As shown in Table 2, the corrosion resistance indexes of Zn15Al are almost more outstanding than those of Zn, which is in a good agreement with the result of the potentiodynamic polarization natural immersion tests.

## 4 Conclusions

1) Three kinds of single layer coatings of Zn, Zn15Al, 316L stainless steel and two kinds of double layer coatings with inner layer of Zn or Zn15Al and outer layer of 316L were developed by arc spraying to protect the metal ends of PHC pipe piles against soil corrosion.

2) The corrosion of the matrix Q235 steel is effectively inhibited by Zn, Zn15Al, Zn+316L and Zn15Al+316L coatings and white rusts were merely observed after immersion for 110 d; but the red rusts presented on 316L coated samples after immersion for one day. The outer layer of 316L for the double layer coatings bubbled and warped after immersion for 30 d.

3) The corrosion rate value of Zn15Al coated samples is negative; that of Zn coated samples is decreased with immersion time; but that of 316L coated samples is increased.

4) The corrosion products of Zn and Zn15Al

become more and more thick and compact with corrosion time. The corrosion resistance indexes of both Zn and Zn15Al coated samples are significantly improved with corrosion time, and those of Zn15Al are more outstanding than those of Zn.

5) When the metal coatings were sealed with epoxy resin, the appearance of the whole coatings almost keep unchanged after immersion for 110 d. Metal arc spraying, especially Zn and Zn15Al coatings, and epoxy resin sealing are remarkably effective to protect the metal ends of PHC pipe piles against chloride salt soil corrosion.

## References

- [1] FISHER A K, BULLEN F, BEAL D. The durability of cellulose fibre reinforced concrete pipes in sewage applications [J]. *Cement and Concrete Research*, 2001, 31(4): 543–553.
- [2] MIYATA Y, NAKANO H, ABE M, AKUTAGAWA H, HAMADA H. Effectiveness of polyethylene coating for steel pipe piles [J]. *Materials Performance*, 2006, 45(12): 24–27.
- [3] DEAN M B. Electrochemical and galvanic corrosion of coated steel surfaces [J]. *Chemical Engineering*, 1982, 89(13): 109–112.
- [4] DU C W, LI X G, LIANG P, LIU Z Y, JIA G F, CHENG Y F. Effects of microstructure on corrosion of X70 pipe steel in an alkaline soil [J]. *Journal of Materials Engineering and Performance*, 2009, 18(2): 216–220.
- [5] ANON. Thermal spray coatings protect steel structures from corrosion [J]. *Advanced Materials and Processes*, 2007, 165(11): 114–115.
- [6] PAPAVINASAM S, ATTARD M, ARSENEULT B, REVIE R W. State-of-the-art of thermal spray coatings for corrosion protection [J]. *Corrosion Reviews*, 2008, 26(2/3): 105–146.
- [7] ZENG Zhen-su, SAKODA N, TAJIRI T. Corrosion behavior of wire-arc-sprayed stainless steel coating on mild steel [J]. *Journal of Thermal Spray Technology*, 2003, 15(3): 431–437.
- [8] de RINCON O, SANCHEZ M, de ROMERO M, PAZ G, CAMPOS W. Long-term performance of different aluminum alloy designs as sacrificial anodes for rebars [J]. *Revista de Metallurgia (Madrid)*, 2003(S1): 228–234.
- [9] TAJIRI T, ZENG Z. Microstructure and corrosion behavior of arc sprayed stainless steel coatings [C]// Montreal: ASM International, 2000: 697–704.
- [10] LIU Yan, ZHU Zi-xin, CHEN Yong-xiong, XU Bin-shi, MA Shi-ning, LI Zhuo-xin. Electrochemical corrosion behavior of arc sprayed Zn-Al coatings [J]. *Trans Nonferrous Met Soc China*, 2004, 14(S1): 443–445.
- [11] CACHET C, GANNE F, JOIRET S, MAURIN G, PETITJEAN J, VIVIER V, WIART R. EIS investigation of zinc dissolution in aerated sulphate medium. Part II: Zinc coatings [J]. *Electrochimica Acta*, 2002, 47(21): 3409–3422.
- [12] CAO Chu-nan, ZHANG Jian-qing. An introduction to electrochemical impedance spectroscopy [M]. Beijing: Science Press, 2002: 24–32. (in Chinese)
- [13] WENG D, JOKIEL P, UEBLEIS A, BOEHNI H. Corrosion and characteristics of zinc and manganese phosphate coatings [J]. *Surface and Coatings Technology*, 1996, 88(1/3): 147–156.
- [14] TANG N, OOIJ W J, GORECKI G. Comparative EIS study of pretreatment performance in coated metals [J]. *Progress in Organic Coatings*, 1997, 30(4): 255–263.
- [15] YAO Jian-ming. College physics (II) [M]. Beijing: Beijing Institute of Technology Press, 2008: 65–72. (in Chinese)

(Edited by YANG Hua)